Molecular Imaging of Pediatric Lymphoma, Sarcomas, and Other Solid Tumors

Yamini Mathur[1] • Kritin Shankar[1] • Hardik Veerwal[1] • Suraj Kumar[1] • Rajender Kumar[1] • Amol M Takalkar[2] • Lance T. Hall[2]

[1]Department of Nuclear Medicine, Post Graduate Institute of Medical Education and Research (PGIMER), Chandigarh, India; [2]Department of Radiology and Imaging Sciences, Emory University, Atlanta, GA, USA

Author for correspondence: Rajender Kumar, Department of Nuclear Medicine, Post Graduate Institute of Medical Education and Research (PGIMER), Chandigarh, India. Email: drrajender2010@gmail.com

Abstract: Pediatric tumors are rare, but often rapidly progressive malignancies which require early diagnosis, accurate staging, and appropriate treatment. Complications due to over treatment or under treatment of pediatric malignancies are a major concern and thus, prompt but pertinent workup along with early treatment response evaluation of tumors is vital. Molecular imaging techniques with positron emission tomography (PET) with computed tomography (PET/CT) and single photon emission computed tomography (SPECT) with CT (SPECT/CT) can often localize and accurately stage pediatric malignancies before morphological changes are evident with anatomical imaging techniques. These findings can help determine the clinical prognosis and treatment plan.

In post-therapy patients, PET/CT and SPECT/CT may more accurately identify or exclude residual/recurrent malignancy. Since pediatric tumors often have overexpression of various molecular pathways, a variety of molecular imaging agents for PET/CT and SPECT/CT can be used (FDG). PET/CT with 18F-FDG usually shows increased tumor uptake in pediatric lymphoma and many other extra-cranial solid tumors. Amino acid based molecular imaging agents can be used in brain tumors and somatostatin receptor (SSTR) peptide molecular imaging agents can be used for tumors of neuroendocrine origin. Ongoing research has developed many novel molecular imaging agents which are in clinical trials.

Keywords: 18F-FDG; molecular imaging; pediatric tumors; PET/CT, radiopharmaceuticals

INTRODUCTION

Cancer incidence rises with age, peaking around the 7th decade, and is less common in the pediatric age group. According to the Global Cancer Observatory, around the 280,000 cancer cases were diagnosed in the age group of (0-19 years) in 2020, with an estimated 110,000 deaths. In contrast to adult malignancies which usually develop from mature tissue, childhood cancers usually originate from developing and growing tissues; hence, they often rapidly progress over weeks to months. Leukemia (25%), brain tumors (17%), lymphoma (16%) and solid tumors such as soft tissue sarcomas (7%), neuroblastoma (5%), nephroblastoma (4%) and retinoblastoma (2%), are the most common tumor types in pediatric patients. Childhood cancers have an overall survival rate of 82%, though prompt diagnosis and management are crucial for therapeutic success (1). Additionally, the increased risk of treatment related complications, such as developing a second malignancy due to prior radiotherapy, makes accurate disease diagnosis essential to minimize risk.

Molecular imaging techniques utilizing PET/CT and SPECT/CT involve imaging a radiolabelled molecule that targets a cancer-specific metabolic pathway, receptor, or other molecular process. Additional non-radioactive molecular imaging techniques can utilize magnetic resonance imaging (MRI) or ultrasonography (USG). Functional molecular imaging has progressed by leaps and bounds with advances in PET imaging and the development of hybrid PET/CT and PET/MRI. FDG, the workhorse molecular imaging agent of PET, has contributed significantly to the evaluation of initial staging, response evaluation, restaging, radiation treatment planning and prognostication of most of the pediatric solid malignancies. Many other molecular imaging agents are available to evaluate different biological aspects of tumors and to aid in functional tumor characterization. The mechanism of uptake and utility of various molecular imaging agents are explained in the following section (Table 1). This chapter highlights the role of molecular imaging in evaluating pediatric lymphoma, sarcomas and other common solid tumors.

TABLE 1	List of radiopharmaceuticals with their mechanism of uptake, uses and special considerations			
Physiologic process	Radiopharmaceuticals	Mechanism of uptake	Utility	Comments
Glucose metabolism	18F-fluorodeoxyglucose (FDG)	Glucose analogue. Active uptake via GLUT 1 and gets trapped within the cell post phosphorylation	Lymphoma (HL and NHL), Neuroblastoma, brain tumour, bone and soft tissue tumors.	High sensitivity. Requires fasting for 4-6 hours. Non-specific to differentiate infective and inflammatory processes.
Amino acid analogues	18F-fluoroethyl tyrosine (FET) 11C – Methionine (MET)	L-type amino acid transporters LAT-1 (uptake via active transport).	Brain tumors- Grade of tumours; recurrence vs treatment changes; prognostication	Need for on-site cyclotron for C-11 based radiopharmaceuticals
Somatostatin receptor (SSTR) expression	**PET agents** • 68Ga- DOTA-tyr³-octreotide (DOTA-TOC) • 68Ga-DOTA-tyr³-octreotate (DOTA-TATE) • 68Ga-DOTA-1-Nal³-octreotide (DOTA-NOC) **SPECT agents** • 111In-diethylenetriaminepentaacetic acid (DTPA)-pentetreotide	Affinity for SSTR 2>5>3 Affinity for SSTR 2>4>5 Affinity for SSTR 2>5>3>4 Affinity for SSTR 2>3>5	Neuroblastoma. Pheochromocytomas and paragangliomas.	Need for on-site 68Ge/ 68Ga generator. Possibility of 177Lu/ 90Y labelled PRRT.

TABLE 1 **List of radiopharmaceuticals with their mechanism of uptake, uses and special considerations (Continued)**

Physiologic process	Radiopharmaceuticals	Mechanism of uptake	Utility	Comments
Norepinephrine metabolism	**SPECT agents** 123I/ 131I- meta iodo benzyl guanidine (MIBG) **PET agents** 124I-MIBG 18F- meta-fluoro benzyl guanidine (MFBG) 18F- dihydroxy phenylalanine (DOPA) 18F- dopamine (DPA)	Norepinephrine transporter mediated uptake and stored in neurosecretory granule via VMAT 1 & 2	Neuroblastoma. Pheochromocytomas and paragangliomas. Brain tumors (DPA and DOPA)	Therapeutic potential of 131I-MIBG
Cell membrane biosynthesis	18F-fluoro-choline (FCH) 11C-choline	Accumulated as phosphatidylcholine via choline kinase	Brain tumours: Differentiate low-grade vs. high-grade glioma	
Cellular proliferation	18F- fluoro-thymidine (FLT)	Thymidine analogue	Experimental; Correlates with a grade of tumor/ Ki 67 index.	Limited studies to evaluate its role in pediatric patients

LYMPHOMA

Lymphoma is a malignant proliferative disease originating from the lymphatic system and is one of the leading childhood cancers, with a prevalence of 12–15% (1). It is divided into Hodgkin lymphoma (HL) and non-Hodgkin lymphoma (NHL). Pediatric NHL is more commonly seen in the younger age group, the diagnosis is predominantly made at the median age of 10 years and increasing incidence thereafter (2). HL has a bimodal age distribution with an initial peak at 20–34 years and a later peak in the 80s, according to National Cancer Institute's Surveillance, Epidemiology and End Results (SEER) (1975–2008). The pediatric HL incidence peaks at the age of 12–19 years. The prevalence of HL depends on socioeconomic status and family size, as immune system maturation occurs with exposure to infections. Additionally, immunodeficient state (3), Epstien-Barr virus infection (4), familial history (5), birth characteristics and birth complications predispose to increased risk of pediatric HL (6). Around 99-fold increased risk is seen in monozygotic twins and 7-fold among siblings (7). According to the (SEER), Cancer Statistics Review (CSR), 1975–2017, NHL accounts for 7.5% of pediatric cancers, while HL makes 6.4%. HL is subdivided into classical HL (CHL) and nodular lymphocyte predominant HL (NLPHL). CHL is further subdivided into four subtypes: nodular sclerosis, mixed cellularity, lymphocyte depleted and lymphocyte rich. The most commonly encountered HL subtypes are nodular sclerosis (70%), mixed cellularity (16%) and NLPHL (7%). NHL has various subtypes depending on the cell of origin, with Burkitt lymphoma being the most common subtype.

Pediatric lymphoma typically presents with regional lymphadenopathy, which is firm and rubbery in consistency. Systemic features such as fever (>38.0°C), anorexia, night sweats and significant weight loss (unintentional ≥10% loss of weight within 6 months of diagnosis) can also be seen and are called "B" symptoms which are the result of raised cytokine production and are indirect evidence of aggressive etiology. However, in older children, mediastinal masses can also be seen, which may lead to dyspnea, dysphagia or coughing. Less commonly, a child may present with acute features resulting from the tumor mass effect, tumor infiltration or rapid growth. The diagnosis should be made based on the morphology and immunohistochemistry of the tissue according to the 2017 WHO Classification of Tumours of Haematopoietic and Lymphoid Tissue guidelines. For the accessible sites, excisional/ incisional biopsy is recommended and for inaccessible lesions, core biopsy is suggested instead of FNAC as the hallmark multinucleated Reed Sternberg cells of HL comprise only 0.1–10% of the tumor bulk. The 5-year survival rate for HL and NHL, 98% and 90%, respectively, have improved significantly over the last 40 years with increasing use of early diagnostic investigations and new treatments. However, there is a 14-fold increased cumulative risk of developing secondary life-limiting neoplasms with a 20 to 30-year latency period after receiving radiotherapy and post-treatment complications require a highly patient tailored approach (8). Increased FDG uptake is noted in 97–100% of HL, 91% of overall NHL but slightly less (around 83%) in rare indolent forms of NHL (9). Consequently, FDG-PET remains a highly sensitive and specific modality and the investigation of choice for the staging and response assessment is discussed in detail in the following sections (10).

FDG-PET: Initial staging

FDG-PET/CT showed superior sensitivity and specificity when compared to traditional staging techniques (USG, CT, MRI and bone scintigraphy), i.e. 96.5–98% versus 77–87.5% and 96.5–100% versus 60–98.7%, respectively (11, 12). Furthermore, the initial staging of disease with PET/CT is essential for risk stratification and accurately defining the extent of potential radiation treatment fields when radiotherapy is anticipated. National comprehensive cancer network (NCCN) guidelines recommend an initial staging workup 2–4 weeks before therapy with an FDG-PET/CT or PET/MR (with CT chest to rule out lung involvement) having diagnostic quality contrast-enhanced CT or MR when available Staging of pediatric HL and NHL follows different staging classifications. The active pediatric HL trials such as the European Network for Pediatric Hodgkin Lymphoma, Clinical Trial 2 (EuroNet- PHL-C2) and Children's Oncology Group (COG) use the Lugano modification of the Ann Arbor staging system (Figure 1). However, pediatric NHL staging follows the International Pediatric Non-Hodgkin Lymphoma Staging System (Figure 2). The positive lesion definition in pediatric lymphoma is different from the Lugano criteria, which uses an adult cut-off of size, which is larger than they are for children, and hence NCCN gives the
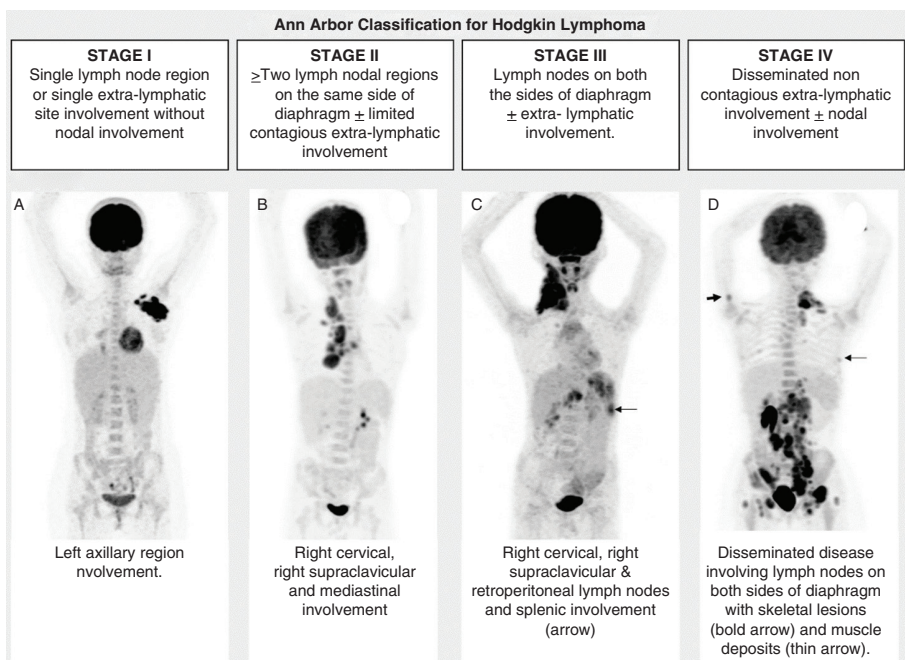

Ann Arbor Classification for Hodgkin Lymphoma			
STAGE I Single lymph node region or single extra-lymphatic site involvement without nodal involvement	**STAGE II** ≥Two lymph nodal regions on the same side of diaphragm ± limited contiguous extra-lymphatic involvement	**STAGE III** Lymph nodes on both the sides of diaphragm ± extra- lymphatic involvement.	**STAGE IV** Disseminated non contagious extra-lymphatic involvement ± nodal involvement
A Left axillary region nvolvement.	B Right cervical, right supraclavicular and mediastinal involvement	C Right cervical, right supraclavicular & retroperitoneal lymph nodes and splenic involvement (arrow)	D Disseminated disease involving lymph nodes on both sides of diaphragm with skeletal lesions (bold arrow) and muscle deposits (thin arrow).

Figure 1. MIP FDG-PET. Ann Arbor classification for HL with examples showing maximum intensity projection (MIP) images of FDG-PET.
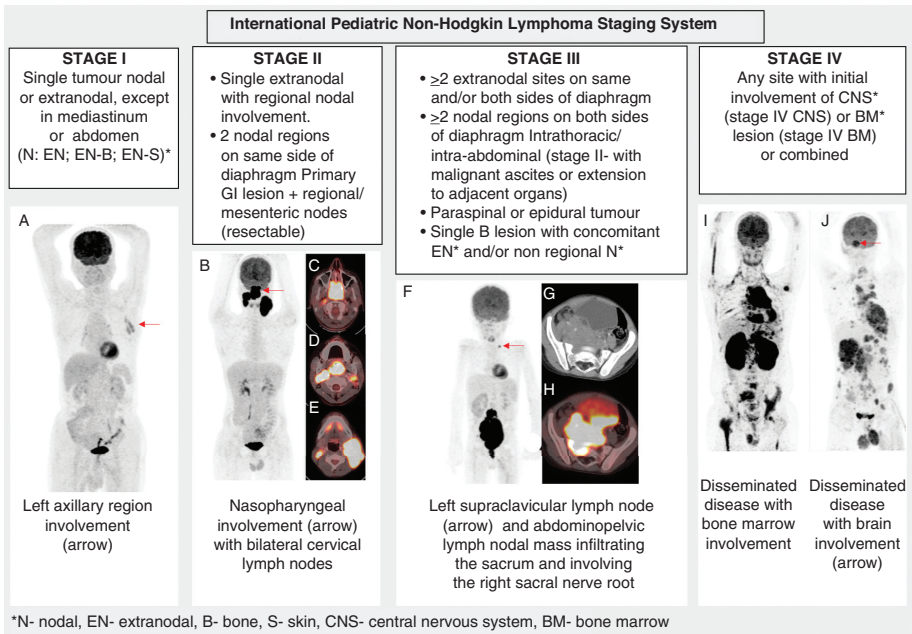
Figure 2. NHL staging system. International Pediatric NHL staging system with examples showing MIP of FDG-PET and cross-sectional PET/CT and CT images.

following protocols for the site involvement based on their panel consensus; however, it is an area for research:

- Lymph node:
  - Long axis diameter (LAD) ≥2cm on CT/MR or
  - LAD is ~1–2cm and the lymph node is FDG-positive on PET/CT

- Spleen:
  - Focal increased FDG uptake that is confirmed on CECT/MRI/USG
  - Splenomegaly with diffuse increased FDG uptake more than the liver is not considered involvement

- Lung:
  - Extra-lymphatic structures (lung lesions) contiguous with nodal masses are considered to be E-lesions
  - At least 1–2 small foci (between 5–10 mm) within the whole lung if no other pathology is suspected
  - At least 1 intrapulmonary focus >1 cm on CT if no other etiology is suspected
  - FDG-positive lesions <1 cm if no other etiology is suspected

Note: If all the lesions are in 1 lung, only it will be considered as involved. However, even if there is a single additional smaller focus within the other lung, both lungs are considered involved.

- Liver:
  - Any focal mass/lesion if no other pathology is suspected
  - Focal FDG-positive lesion

- Bone marrow:
  - ≥3 FDG-positive marrow based lesions.
  - Bone marrow biopsy is not recommended, and diffusely increased bone marrow FDG uptake is not generally considered involvement.

- Bone: FDG-positive lesion with cortical bony destruction on CT or MRI.
- Waldeyer's ring: asymmetrical increased FDG uptake
- Thymus: focal FDG uptake or nodal presentation

    Note: NCCN provides guidelines only for pediatric HL. No separate guidelines are available for pediatric NHL yet.

FDG-PET: Response evaluation

An interim FDG-PET scan is obtained to evaluate the early response to chemotherapy as seen in the EuroNet-PHL-C1 trial, where radiotherapy was omitted in patients with adequate response to 2 cycles of chemotherapy on FDG-PET/CT. The trial showed comparable event-free survival of 88% vs. 87%, with and without radiotherapy, respectively. Thus, the interim PET after 2 cycles of chemotherapy is useful to evaluate the early response and decide the need for radiotherapy and treatment intensification. Response assessment using a semi-objective 5-point scale or Deauville score is now well-established, where score-1 is no abnormal uptake, score-2 is uptake ≤ mediastinal blood pool, score-3 is uptake >blood pool but <liver, score-4 is abnormal uptake >liver and score-5 refers to significant increased FDG uptake as compared to the liver or new site(s) of disease. A score of 1–3 describes a complete metabolic response, but a score of 4/5 suggests the existence of residual or recurrent disease. A Deauville score of 1/2 at least 6 – 8 weeks after the completion of treatment indicates a complete metabolic response. Since FDG-PET shows physiological uptake in the brown adipose tissue and thymus and inflammatory or reactive uptake in bone marrow, spleen, thymus and Waldeyer's ring, the positive predictive value declines. Compared to qualitative interpretation based on scan report, the Deauville score based interpretations have identical negative predictive values of 95.6% and 95.1% but a significantly higher positive predictive value of 72.7% compared to 44.4%, making it more accurate than subjective visual PET interpretations (13).

FDG-PET: Surveillance

FDG-PET scans performed for surveillance (without suspicion of recurrence) are generally not advised due to concern for false-positive results, lack of cost-effective benefit, and undue radiation exposure. Imaging investigations such as X-ray, CT, or MRI are usually advised initially if recurrence is suspected, potentially followed by FDG-PET/CT as clinically warranted.

Role of FDG PET/MRI

FDG-PET/MRI reduces radiation exposure by 50%–75% versus FDG-PET/CT in pediatric lymphoma staging and response evaluation but requires additional time and has limited data for pediatric lymphoma staging and response evaluation (14).

SARCOMAS AND OTHER SOLID TUMORS

Sarcomas represent over one-fifth of all pediatric solid tumors. Rhabdomyosarcoma is the predominant soft tissue sarcoma, while osteosarcoma (OS) and Ewing sarcoma (ES) are the predominant osseous sarcoma (15). Other frequently encountered solid malignancies include neuroblastoma, Wilms tumor, germ cell tumors (GCT), retinoblastoma (RB) and hepatoblastoma. The following section will examine the role of molecular imaging in frequently encountered pediatric solid tumors.

Neuroblastoma

Neuroblastomas are derived from the sympatho-renal lineage of neural crest cells. They account for 8% of total pediatric cancers. They are seen along the sympathetic chain, with the most common site in the adrenal glands, followed by the retroperitoneum and the mediastinum. Almost half of the patients have distant metastases, commonly involving the bone and lymph nodes at initial presentation.

The International Neuroblastoma Risk Group staging system (INRGSS) and International Neuroblastoma staging system (INSS) are used for pre and post-surgical staging, respectively. Accurate determination of the extent of disease is essential as these scoring systems are also utilized for risk-based neuroblastoma patient stratification.

Conventional anatomic and molecular imaging techniques are crucial in initial staging, treatment response, and surveillance. MRI is preferred for locoregional staging due to its excellent anatomical resolution and ability to visualize the intraspinal extension of the disease. 123I-MIBG imaging is the preferred SPECT imaging agent for detecting distal metastases. PET imaging agents used are FDG, DOTA peptides, DOPA and a few novel agents such as mFBG and 11C-mHED PET/CT.

123I- or 131I-MIBG imaging is recommended for detecting distal metastases during initial staging and for initial assessment and follow-up of patients receiving 131I-MIBG therapy. The reported sensitivity and specificity of MIBG for detecting neuroblastoma are 88% and 83%, respectively (16). Semi-quantitative scoring systems have been developed for MIBG scans. Curie system (developed by COG) divides the skeleton into 9 segments and an additional 10th compartment for soft tissue lesions. Each compartment is given a score from 0 to 3 based on the extent of the involvement of the compartment. The International Society of Paediatric Oncology European Neuroblastoma Group (SIOPEN) divides the body into 12 segments, each with a score from 0 to 6 (17) (Figure 3). FDG and 123I-MIBG are
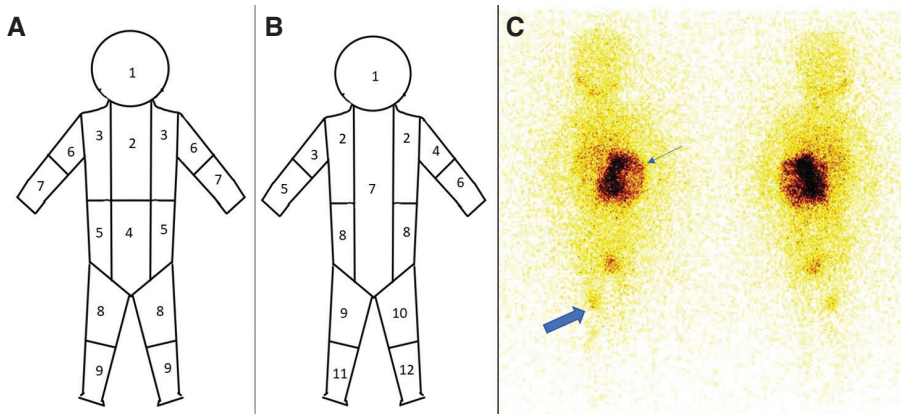
Figure 3. MIBG Scans. (A) Curie and **(B)** SIOPEN scoring systems for MIBG scans. A 10-year-old male patient with a history of left lumbar region neuroblastoma. Anterior and posterior whole body 131I-MIBG scan shows MIBG-avid primary lesion in the left retroperitoneum region (arrow) with tracer avid skeletal lesion in the mid-shaft of the right femur (solid arrow). This patient has a single focus of skeletal uptake in a single segment and > 50% involvement of two of the abdominal segments; thus, Curie and SIPOEN scoring will be 7.

considered complementary imaging, each potentially demonstrating disease not detected by the other. FDG-PET/CT has shown better sensitivity and specificity when used as a complementary imaging modality, with reported sensitivity and specificity being 78% and 92%, respectively (18). Therefore, patients with non-MIBG avid neuroblastomas are subject to an FDG-PET/CT. FDG-PET/CT has also been utilized for assessing the prognosis of the patient.

DOPA accumulates in cells with increased catecholamine activity and therefore is a good alternative to MIBG for detecting tumors derived from neural crest cells, including neuroblastoma. Studies have reported better accuracy of DOPA in comparison to 123I-MIBG (19,20). A recent study has reported the sensitivity and specificity of DOPA to be 86% and 99%, respectively, for detecting soft tissue and bone or bone-marrow metastases in neuroblastoma (21).

Approximately 90% of neuroblastoma tumors express SSTR making DOTA peptides highly sensitive and specific for its detection (22). Patients with high DOTA peptide avidity are also potential candidates for Peptide Receptor Radionucleotide Therapy (PRRT).

Various novel molecular imaging agents are currently under investigation, such as 11C-mHED, a norepinephrine analog and 18F-floropropylbenzylguanidine (FPBG), an analog of benzyl guanidine. They localize within the tumor cells utilizing the same physiologic process involved with DOPA.

Pheochromocytomas and paragangliomas (PPGL)

Paragangliomas are a group of tumors that arise from the autonomic nervous system. PPGLs arising from the adrenal medulla are called pheochromocytomas. They have an incidence rate of 0.2–0.3 cases per million (23). These tumors

secrete catecholamines like epinephrine, norepinephrine and dopamine, which can precipitate life-threatening complications. Approximately 10% of the cases of pheochromocytoma and paraganglioma can be multifocal. Multifocality is often associated with hereditary syndromes such as von Hippel-Lindau (VHL) and multiple endocrine neoplasia (MEN) syndromes.

PPGLs are staged based on the TNM staging system. Tumor (T) staging depends upon the size: T1 < 5cm, T2 > 5 cm, and T3 when the tumor invades the surrounding tissue. Nodal staging (N) is N0 – no regional lymph nodes and N1-regional lymph nodes are involved. Metastasis (M) staging is M0 – no distant metastasis and M1 – metastasis is detected (M1a – metastasis to the bone only, M1b – metastasis to distant lymph nodes, liver or lung and M1c – distant metastasis to bone and multiple other sites.

CT and MRI are the preferred imaging modalities for loco-regional disease assessment. An adrenal lesion with an average Hounsfield unit (HU) of less than 10 on a non-contrast CT image is usually excluded from the suspicion of being a pheochromocytoma (24). Molecular imaging is often used in the clinical diagnosis and management of these patients, utilizing molecular imaging agents such as 123I-MIBG, DOTA peptide, DOPA and FDG.

A meta-analysis has reported the sensitivity and specificity of 123I-MIBG to be 98% and 98%, respectively, for identifying lesions in the adrenal gland and 98% and 79%, respectively, for localizing metastases (25). However, with the increasing use of newer molecular imaging agents, the importance of MIBG in the workup of pheochromocytoma and paraganglioma is steadily decreasing. Another SPECT agent occasionally used for bone scans is 99mTc-methylene diphosphonate (MDP). This binds to hydroxyapatite crystals at sites with increased osteoblastic activity and is useful in identifying active skeletal metastasis. The use of MDP bone scan in the workup of neuroblastoma and PPGLs is decreasing due to suboptimal specificity for osseous metastases along with the availability of newer PET agents.

FDG, DOPA, and DOTA peptides are currently the predominant PET molecular imaging agents used in PPGL assessment. The reported sensitivity and specificity in a meta-analysis of FDG-PET/CT for detecting metastatic pheochromocytomas and paragangliomas with germline mutations is 85% and 65%, respectively (26). Studies have reported good FDG avidity in PPGLs, especially in metastases with succinate dehydrogenase complex iron sulfur subunit B (SDHB) mutation. However, PPGLs with associated MEN 2 syndrome and head and neck PGLs are usually not very FDG-avid. DOPA PET/CT has shown high sensitivity and specificity in detecting pheochromocytoma/paraganglioma compared to SPECT with agents such as MIBG. The sensitivity and specificity of DOPA are reported to be around 79% and 95%, respectively (27). Due to its negligible physiological uptake in the adrenal glands, 18F-DOPA has an advantage over other agents and can be used to detect small lesions.

DOTA peptides are seen to be highly sensitive in the detection of PPGLs, with the pooled detection rate of PPGLs in a recent systemic review reported as 93%, which exceeds the detection rate of DOPA and FDG (28). However, uptake in meningioma, inflammatory disease and a few other cancers can give false positive results (29).

Recent pheochromocytoma and paraganglioma guidelines by EANM recommend using specific agents in various scenarios. DOPA PET/CT is the preferred

molecular imaging agent for sporadic and inherited pheochromocytomas, except for ones showing succinate dehyrogenase (SDHx) mutations. In cases of extra-adrenal sympathetic/multifocal/metastatic/SDHx mutants and head and neck PGLs, DOTA peptides are the preferred PET molecular imaging agents.

Novel molecular imaging agents

11C-mHED is a norepinephrine analog. Due to its rapid accumulation within the lesion and faster background clearance, imaging can be done within 30 minutes. However, the use of this agent is limited due to its short half-life of 11C, which is 20 minutes. Few benzyl guanidine analogs have been tried for imaging, such as 18F-FPBG. A study by Samim et al. reported 2 extra lesions detected per patient in the FPBG scan compared to the MIBG scan (30).

Osteosarcoma (OS)

Osteosarcoma is an osseous neoplasm that leads to the deposition of malignant osteoid from atypical osteoblasts. It is the most prevalent pediatric bone cancer, with the highest peak incidence in children and adolescents and another peak incidence in individuals over 60 years. Treatment for localized OS typically involves high-dose chemotherapy and limb-salvage surgery when appropriate. A significant proportion of patients present with metastases, more commonly in the lungs and bones and rarely to the lymph nodes. Early detection of metastatic disease is crucial for risk stratification and treatment. Historically, initial evaluation for skeletal metastasis in OS was performed by radionuclide skeletal scintigraphy (SSC) using 99mTc-labelled diphosphonates, commonly 99mTc-MDP. Although its cost-effectiveness and high sensitivity make it attractive, SSC is limited by its relatively low specificity, spatial resolution and image quality. Current research demonstrates the advantage of FDG-PET/CT over SSC in evaluating bone metastases. FDG-PET/CT is a highly sensitive diagnostic tool, with a meta-analysis of 26 studies by Liu F et al. demonstrating 100% sensitivity for detecting the primary tumor. The same study also showed a sensitivity of 72–88%, 87–97% and 86–93% and a specificity of 89–97%, 96–98% and 95–97% for the diagnosis of lung, bone and all distant metastases respectively (31). It is also crucial to detect early recurrence after limb salvage surgery, which occurs in around 13% of patients. The meta-analysis displayed a sensitivity of 81–96% and a specificity of 87–97% for recognizing recurrent OS. However, the utility of FDG-PET/CT is comparable or slightly inferior to CT for lung nodule evaluation. Patients with OS generally receive neoadjuvant chemotherapy before local control surgery, with >90% tumor necrosis suggesting a favorable response to chemotherapy and improved outcomes compared to tumors with a poor histological response. FDG-PET has also correlated with histological response to chemotherapy and predicting tumor necrosis. PET-derived semi-quantitative parameters such as peak and maximum standardized uptake value (SUVpeak and SUVmax), metabolic tumor volume (MTV), and total lesion glycolysis (TLG) are predictive of overall survival and event-free survival and hence, can serve as useful prognostic biomarkers in OS (32).

Ewing sarcoma (ES)

The Ewing family of tumors is a group of small round blue cell neoplasms originating in bone, soft tissues, or visceral sites and sharing a common genetic alteration, t(11;22)(q24;q12), in over 85% of cases. At the time of diagnosis, around 25% of patients with ES have detectable metastases, predominantly in the lung and bone/bone marrow (33). Metastatic assessment typically involves a CT chest for pulmonary metastasis, bone marrow aspiration and biopsy for bone marrow involvement, ^{99m}Tc-MDP SSC for osseous metastasis, and FDG-PET/CT. As metastases from ES are frequently osteolytic and may involve the bone marrow, SSC may have limited sensitivity. FDG-PET/CT has demonstrated high sensitivity (80–92%) and specificity (86–96%) for bone and bone marrow metastases in ES (34). Bone marrow biopsy can also be inferior to FDG-PET as the former may be performed from uninvolved sites (35). Furthermore, as with OS, semi-quantitative parameters derived from FDG-PET can correlate with microscopic chemotherapeutic response and progression-free survival and serve as prognostic indices in ES (36).

Rhabdomyosarcoma (RMS)

Rhabdomyosarcoma, a highly aggressive tumor, originates from primitive mesenchymal cells showing variable skeletal muscle differentiation. RMS frequently involves the head, skull, neck, urinary bladder or prostate. At the time of diagnosis, one-fifth of cases can demonstrate distant spread to the lungs, skeleton, marrow or lymph nodes. A retrospective review of a study performed by the European pediatric Soft tissue sarcoma Study Group (EpSSG) dedicated to metastatic RMS aimed to determine the value of PET/CT in staging the disease. Compared to standard anatomic imaging workup, molecular imaging with PET/CT was superior in detecting loco-regional (96.2% vs. 78.5%) and distant (94.8% vs. 79.3%) lymph nodes. The sensitivity of PET/CT was also greater than SSC (96.4% vs. 67.9%) for bone metastases and could detect marrow involvement with a sensitivity of 91.8% and specificity of 93.8%. However, it was lower in sensitivity for lung metastases than CT chest (79.6% vs. 100%) (37).

Wilms tumor (Nephroblastoma)

Wilms tumor is the most frequent malignancy of embryonal origin arising from the kidneys in children. Histologically, it can demonstrate a favorable histology consisting of a triphasic pattern of blastema, epithelial, and stromal tissues or an unfavorable pattern displaying a higher degree of anaplasia. It can be associated with specific syndromes such as Wilms tumor, aniridia, genitourinary anomalies, range of developmental delays (WAGR) syndrome, Denys-Drash syndrome, and Beckwith-Wiedemann syndrome. Imaging studies are performed to characterize the extent of the primary lesion, regional lymph node involvement and assess for pulmonary or less commonly osseous metastases. Limited literature is available thus far on the utility of FDG-PET/CT in Wilms tumor. Most studies have demonstrated FDG avidity in Wilms tumor with the

degree of differentiation correlating well with SUV. These studies suggest that FDG-PET/CT can be useful in initial staging, assessing chemotherapy response, and detecting recurrent disease (38).

Germ cell tumors (GCTs)

GCTs are a heterogeneous tumor group arising from precursor germ cells. They are divided into gonadal or extragonadal in location, with extragonadal GCT frequently occurring in the midline (mediastinal, retroperitoneal, and sacrococcygeal). GCT varies on the differentiation degree into mature (with a relatively benign course) or immature teratomas and malignant GCT. With a lower rate of glycolysis, mature teratomas tend to exhibit lesser FDG uptake. Though FDG-PET/CT does not yet have a completely established role in GCTs, studies have exhibited its potential in immature teratomas and malignant GCTs (39). Though its performance may be comparable to conventional imaging in the initial evaluation, it can be particularly beneficial in patients after therapy to identify residual or recurrent disease (40).

Retinoblastoma (RB)

RB is the intraocular cancer with the highest incidence in the pediatric population. RB can be present bilaterally if associated with a germline mutation in the RB-1 gene on chromosome 13q14. It can present with leukocoria or strabismus and early disease detection carries a favorable prognosis. However, a delay in diagnosis, particularly in low-middle-income countries, can lead to the development of locally advanced RB with either microscopic or macroscopic spread beyond the ocular globe and a high risk for metastatic disease. RB can spread to the orbit via the optic sheath, meninges, or distantly through hematogenous dissemination. To evaluate the local or intracranial spread of the disease, diagnostic imaging can be performed by USG, CT or MRI. Children with a risk for metastases can be screened through SSC. The limited literature on PET/CT has endorsed the utility of FDG uptake in the optic nerve in predicting event-free survival and overall survival after neoadjuvant chemotherapy (41). A negative FDG-PET after the completion of treatment in patients with equivocal MRI findings has also aided in avoiding further unnecessary treatment (42). FDG-PET/MRI may be potentially useful for evaluating RB, but more data is awaited.

Langerhans cell histiocytosis (LCH)

LCH is a rare clonal proliferative disorder with 3–5 per million incidences. It involves the histiocytes, a specialized antigen-presenting cell found in the epidermis, mucosa, and lymph nodes. LCH can have a varied presentation ranging from benign single site disease to multi-systemic disease (43). LCH is classified into a single system with a single site or multiple site involvement or multisystem with or without organ (liver, spleen, bone marrow, CNS) involvement. Accurate pretreatment staging is important as the treatment varies from local excision for localized disease to prolonged chemotherapy for multi-systemic disease. FDG-PET/CT is seen to have sensitivity (100%) and specificity (83%) in the initial evaluation

of the extent of the disease and can accurately demonstrate a response to treatment (44). In addition to LCH, FDG-PET/CT also plays a role in assessing other histiocytic disorders such as Erdheim Chester disease, Rosai Dorfman disease, Xantho-granulomas and malignant histiocytosis. Various guidelines, including the NCCN, recommend a Head-to-toe PET/CT for initial evaluation and response assessment in LCH and ECD. It is also recommended for post-treatment surveillance every 6 months for 2 years in patients with LCH (45).

CONCLUSION

Molecular imaging has revolutionized the management of pediatric cancers with accurate early diagnosis, tumor characterization, risk stratification, identifying the most aggressive site for biopsy, early treatment response assessment and differentiating post-treatment changes from tumor recurrence/relapse of disease. It has helped treatment planning and medication, depending on the extent of staging and interim response, which can help reduce the risk of treatment-related complications, including secondary malignancies. Beyond the diagnostic purview, DOTA peptides and 123I-MIBG are also used for targeted radionuclide therapy planning (177Lu-PRRT and 131I-MIBG) in solid tumors of neuroendocrine origin. The recent introduction of PET/MRI has led to better delineation of the soft tissue, marrow based and CNS lesions with significantly low radiation dose; however, further clinical trials are required to establish and compare its role in different pediatric malignancies.

Conflict of Interest: The authors declare that they have no potential conflict of interest with respect to the research, authorship, and/or publication of this chapter.

Copyright and Permission Statement: The authors confirm that the materials included in this chapter do not violate copyright laws. Where relevant, appropriate permissions have been obtained from the original copyright holder(s), and all original sources have been appropriately acknowledged or referenced. Where relevant, informed consent has been obtained from patients or their caregivers according to applicable national or institutional policies.

REFERENCES

1. Institute of Medicine (US) and National Research Council (US) National Cancer Policy Board. Childhood Cancer Survivorship: Improving Care and Quality of Life [Internet]. Hewitt M, Weiner SL, Simone JV, editors. Washington (DC): National Academies Press (US); 2003 [cited 2023 May 7]. Available from: http://www.ncbi.nlm.nih.gov/books/NBK221742/
2. Kaatsch P. Epidemiology of childhood cancer. Cancer Treat Rev. 2010;36(4):277–285. https://doi.org/10.1016/j.ctrv.2010.02.003
3. Robison LL, Stoker V, Frizzera G, Heinitz K, Meadows AT, Filipovich AH. Hodgkin's disease in pediatric patients with naturally occurring immunodeficiency. Am J Pediatr Hematol Oncol. 1987;9(2):189–192. https://doi.org/10.1097/00043426-198722000-00019

4. Bräuninger A, Schmitz R, Bechtel D, Renné C, Hansmann ML, Küppers R. Molecular biology of Hodgkin's and Reed/Sternberg cells in Hodgkin's lymphoma. Int J Cancer. 2006;118(8):1853–1861. https://doi.org/10.1002/ijc.21716

5. Ferraris AM, Racchi O, Rapezzi D, Gaetani GF, Boffetta P. Familial Hodgkin's disease: a disease of young adulthood?. Ann Hematol. 1997;74(3):131–134. https://doi.org/10.1007/s002770050270

6. Chun GYC, Sample J, Hubbard AK, Spector LG, Williams LA. Trends in pediatric lymphoma incidence by global region, age and sex from 1988–2012. Cancer Epidemiol. 2021 Aug;73:101965. https://doi.org/10.1016/j.canep.2021.101965

7. Lanzkowsky, P. (2011). Hodgkin Lymphoma. Manual of Pediatric Hematology and Oncology, 599–623. doi:10.1016/b978-0-12-375154-6.00019-7https://doi.org/10.1016/B978-0-12-375154-6.00019-7

8. Holmqvist AS, Chen Y, Berano Teh J, Sun C, Birch JM, van den Bos C, et al. Risk of solid subsequent malignant neoplasms after childhood Hodgkin lymphoma-Identification of high-risk populations to guide surveillance: A report from the Late Effects Study Group. Cancer. 2019 Apr 15;125(8):1373–83. https://doi.org/10.1002/cncr.31807

9. Weiler-Sagie M, Bushelev O, Epelbaum R, Dann EJ, Haim N, Avivi I, et al. (18)F-FDG avidity in lymphoma readdressed: a study of 766 patients. J Nucl Med Off Publ Soc Nucl Med. 2010 Jan;51(1):25–30. https://doi.org/10.2967/jnumed.109.067892

10. London K, Cross S, Onikul E, Dalla-Pozza L, Howman-Giles R. 18F-FDG PET/CT in paediatric lymphoma: comparison with conventional imaging. Eur J Nucl Med Mol Imaging. 2011 Feb;38(2):274–84. https://doi.org/10.1007/s00259-010-1619-6

11. Kabickova E, Sumerauer D, Cumlivska E, Drahokoupilova E, Nekolna M, Chanova M, et al. Comparison of 18F-FDG-PET and standard procedures for the pretreatment staging of children and adolescents with Hodgkin's disease. Eur J Nucl Med Mol Imaging. 2006 Aug 11;33(9):1025–31. https://doi.org/10.1007/s00259-005-0019-9

12. Hernandez-Pampaloni M, Takalkar A, Yu JQ, Zhuang H, Alavi A. F-18 FDG-PET imaging and correlation with CT in staging and follow-up of pediatric lymphomas. Pediatr Radiol.

13. Sedig LK, Bailey JJ, Wong KK, Brown RKJ, Kaminski MS, Hutchinson RJ. Do Deauville Scores Improve the Clinical Utility of End-of-Therapy FDG PET Scans for Pediatric Hodgkin Lymphoma? AJR Am J Roentgenol. 2019 Feb;212(2):456–60. https://doi.org/10.2214/AJR.18.19755

14. Gatidis S, Schmidt H, la Fougère C, Nikolaou K, Schwenzer NF, Schäfer JF. Defining optimal tracer activities in pediatric oncologic whole-body 18F-FDG-PET/MRI. Eur J Nucl Med Mol Imaging. 2016 Dec;43(13):2283–9. https://doi.org/10.1007/s00259-016-3503-5

15. Steliarova-Foucher E, Colombet M, Ries LAG, Moreno F, Dolya A, Bray F, et al. International incidence of childhood cancer, 2001-10: a population-based registry study. Lancet Oncol. 2017 Jun;18(6):719–31.

16. Terry A. Vik M, Thomas Pfluger M, Richard Kadota et al. 123I-mIBG Scintigraphy in Patients With Known or Suspected Neuroblastoma: Results From a Prospective Multicenter Trial. Pediatr Blood Cancer. 2013;(February):1388–9.

17. Sharp SE, Trout AT, Weiss BD, Gelfand MJ. MIBG in neuroblastoma diagnostic imaging and therapy. Radiographics. 2016;36(1):258–78. https://doi.org/10.1148/rg.2016150099

18. Melzer HI, Coppenrath E, Schmid I, Albert MH, von Schweinitz D, Tudball C, et al. 123I-MIBG scintigraphy/SPECT versus 18F-FDG PET in paediatric neuroblastoma. Eur J Nucl Med Mol Imaging. 2011;38(9):1648–58. https://doi.org/10.1007/s00259-011-1843-8

19. Piccardo A, Lopci E, Conte M, Garaventa A, Foppiani L, Altrinetti V, et al. Comparison of 18F-dopa PET/CT and 123I-MIBG scintigraphy in stage 3 and 4 neuroblastoma: A pilot study. Eur J Nucl Med Mol Imaging. 2012 Jan 20;39(1):57–71. https://doi.org/10.1007/s00259-011-1938-2

20. Fiebrich HB, Brouwers AH, Kerstens MN, Pijl MEJ, Kema IP, De Jong JR, et al. 6-[F-18]fluoro-L-dihydroxyphenylalanine positron emission tomography is superior to conventional imaging with 123I-metaiodobenzylguanidine scintigraphy, computer tomography, and magnetic resonance imaging in localizing tumors causing catecholamine excess. J Clin Endocrinol Metab. 2009;94(10):3922–30. https://doi.org/10.1210/jc.2009-1054

21. Piccardo A, Morana G, Puntoni M, Campora S, Sorrentino S, Zucchetta P, et al. Diagnosis, Treatment Response, and Prognosis: The Role of 18F-DOPA PET/CT in Children Affected by Neuroblastoma in Comparison with 123I-mIBG Scan: The First Prospective Study. J Nucl Med. 2020 Mar 1;61(3):367 LP - 374. https://doi.org/10.2967/jnumed.119.232553

22. Watanabe N, Nakanishi Y, Kinukawa N, Ohni S, Obana Y, Nakazawa A, et al. Expressions of somatostatin receptor subtypes (SSTR-1, 2, 3, 4 and 5) in neuroblastic tumors; special reference to clinicopathological correlations with International Neuroblastoma Pathology Classification and outcomes. Acta Histochem Cytochem. 2014;47(5):219–29. https://doi.org/10.1267/ahc.14024

23. Park H, Kim MS, Lee J, Kim JH, Jeong BC, Lee S, et al. Clinical Presentation and Treatment Outcomes of Children and Adolescents With Pheochromocytoma and Paraganglioma in a Single Center in Korea. Front Endocrinol (Lausanne). 2021;11(January):1–7. https://doi.org/10.3389/fendo.2020.610746

24. Park JJ, Park BK, Kim CK. Adrenal imaging for adenoma characterization: Imaging features, diagnostic accuracies and differential diagnoses. Br J Radiol. 2016;89(1062):1–13. https://doi.org/10.1259/bjr.20151018

25. Van Der Horst-Schrivers ANA, Jager PL, Boezen HM, Schouten JP, Kema IP, Links TP. Iodine-123 metaiodobenzylguanidine scintigraphy in localising phaeochromocytomas - Experience and meta-analysis. Anticancer Res. 2006;26(2 B):1599–604.

26. Kan Y, Zhang S, Wang W, Liu J, Yang J, Wang Z. 68Ga-somatostatin receptor analogs and 18F-FDG PET/CT in the localization of metastatic pheochromocytomas and paragangliomas with germline mutations: a meta-analysis. Acta radiol. 2018;59(12):1466–74. https://doi.org/10.1177/0284185118764206

27. Treglia G, Cocciolillo F, De Waure C, Di Nardo F, Gualano MR, Castaldi P, et al. Diagnostic performance of 18F-dihydroxyphenylalanine positron emission tomography in patients with paraganglioma: A meta-analysis. Eur J Nucl Med Mol Imaging. 2012;39(7):1144–53. https://doi.org/10.1007/s00259-012-2087-y

28. Han S, Suh CH, Woo S, Kim YJ, Lee JJ. Performance of 68 Ga-DOTA-conjugated somatostatin receptor-targeting peptide PET in detection of pheochromocytoma and paraganglioma: A systematic review and meta-analysis. J Nucl Med. 2019;60(3):369–76. https://doi.org/10.2967/jnumed.118.211706

29. Skoura E, Michopoulou S, Mohmaduvesh M, Panagiotidis E, Al Harbi M, Toumpanakis C, et al. The impact of 68Ga-DOTATATE PET/CT imaging on management of patients with neuroendocrine tumors: Experience from a national referral center in the United Kingdom. J Nucl Med. 2016;57(1):34–40. https://doi.org/10.2967/jnumed.115.166017

30. Samim A, Blom T, Poot AJ, Windhorst AD, Fiocco M, Tolboom N, et al. [18F]mFBG PET-CT for detection and localisation of neuroblastoma: a prospective pilot study. Eur J Nucl Med Mol Imaging. 2023;50(4):1146–57. https://doi.org/10.1007/s00259-022-06063-6

31. Liu F, Zhang Q, Zhou D, Dong J. Effectiveness of 18F-FDG PET/CT in the diagnosis and staging of osteosarcoma: a meta-analysis of 26 studies. BMC Cancer. 2019 Dec;19(1):323. https://doi.org/10.1186/s12885-019-5488-5

32. Im HJ, Zhang Y, Wu H, Wu J, Daw NC, Navid F, et al. Prognostic Value of Metabolic and Volumetric Parameters of FDG PET in Pediatric Osteosarcoma: A Hypothesis-generating Study. Radiology. 2018 Apr;287(1):303–12. https://doi.org/10.1148/radiol.2017162758

33. Bernstein ML, Devidas M, Lafreniere D, Souid AK, Meyers PA, Gebhardt M, et al. Intensive therapy with growth factor support for patients with Ewing tumor metastatic at diagnosis: Pediatric Oncology Group/Children's Cancer Group Phase II Study 9457--a report from the Children's Oncology Group. J Clin Oncol. 2006 Jan 1;24(1):152–9. https://doi.org/10.1200/JCO.2005.02.1717

34. Huang T, Li F, Yan Z, Ma Y, Xiong F, Cai X, et al. Effectiveness of 18F-FDG PET/CT in the diagnosis, staging and recurrence monitoring of Ewing sarcoma family of tumors: A meta-analysis of 23 studies. Medicine (Baltimore). 2018 Nov;97(48):e13457. https://doi.org/10.1097/MD.0000000000013457

35. Kasalak Ö, Glaudemans AWJM, Overbosch J, Jutte PC, Kwee TC. Can FDG-PET/CT replace blind bone marrow biopsy of the posterior iliac crest in Ewing sarcoma? Skeletal Radiol. 2018 Mar;47(3):363–7. https://doi.org/10.1007/s00256-017-2807-2

36. Annovazzi A, Ferraresi V, Anelli V, Covello R, Vari S, Zoccali C, et al. [18F]FDG PET/CT quantitative parameters for the prediction of histological response to induction chemotherapy and clinical outcome in patients with localised bone and soft-tissue Ewing sarcoma. Eur Radiol. 2021 Sep 1;31(9):7012–21. https://doi.org/10.1007/s00330-021-07841-w

37. Mercolini F, Zucchetta P, Jehanno N, Corradini N, Van Rijn RR, Rogers T, et al. Role of 18F-FDG-PET/CT in the staging of metastatic rhabdomyosarcoma: a report from the European paediatric Soft tissue sarcoma Study Group. European Journal of Cancer. 2021 Sep;155:155–62. https://doi.org/10.1016/j.ejca.2021.07.006

38. Begent J, Sebire NJ, Levitt G, Brock P, Jones KP, Ell P, et al. Pilot study of F18-Fluorodeoxyglucose Positron Emission Tomography/computerised tomography in Wilms' tumour: Correlation with conventional imaging, pathology and immunohistochemistry. European Journal of Cancer. 2011 Feb 1;47(3):389–96. https://doi.org/10.1016/j.ejca.2010.09.039

39. De Giorgi U, Pupi A, Fiorentini G, Rosti G, Marangolo M. FDG-PET in the management of germ cell tumor. Annals of Oncology. 2005 May;16:iv90-4. https://doi.org/10.1093/annonc/mdi915

40. Hart A, Vali R, Marie E, Shaikh F, Shammas A. The clinical impact of 18F-FDG PET/CT in extracranial pediatric germ cell tumors. Pediatr Radiol. 2017 Oct 1;47(11):1508–13. https://doi.org/10.1007/s00247-017-3899-5

41. Radhakrishnan V, Kumar R, Malhotra A, Bakhshi S. Role of PET/CT in Staging and Evaluation of Treatment Response After 3 Cycles of Chemotherapy in Locally Advanced Retinoblastoma: A Prospective Study. Journal of Nuclear Medicine. 2012 Feb 1;53(2):191–8. https://doi.org/10.2967/jnumed.111.095836

42. Moothedath AW, Chopra KK, Seth R, Meena JP, Gupta AK, Kumar R, et al. Role of 18-Fluorodeoxyglucose Positron Emission Tomography-Computed Tomography in Predicting Residual Disease Posttreatment Completion in Retinoblastoma Patients. Indian J Nucl Med. 2022;37(2):142–6. https://doi.org/10.4103/ijnm.ijnm_145_21

43. Badalian-Very G, Vergilio JA, Fleming M, Rollins BJ. Pathogenesis of Langerhans Cell Histiocytosis. Annu Rev Pathol Mech Dis. 2013 Jan 24;8(1):1–20. https://doi.org/10.1146/annurev-pathol-020712-163959

44. Jessop S, Crudgington D, London K, Kellie S, Howman-Giles R. FDG PET-CT in pediatric Langerhans cell histiocytosis. Pediatr Blood Cancer. 2020 Jan;67(1):e28034. https://doi.org/10.1002/pbc.28034

45. Go RS, Jacobsen E, Baiocchi R, Buhtoiarov I, Butler EB, Campbell PK, et al. Histiocytic Neoplasms, Version 2.2021, NCCN Clinical Practice Guidelines in Oncology. Journal of the National Comprehensive Cancer Network. 2021 Nov 1;19(11):1277–303. https://doi.org/10.6004/jnccn.2021.0053